International Journal of Science and Research (IJSR)
ISSN: 2319-7064
Index Copernicus Value (2016): 79.57 | Impact Factor (2017): 7.296

pH Sensitivity of Screen-Printed Sensors based Onamorphous and Crystalline RuO_2 and the Impact of Conducting and Inert Binders

S. Chalupczok*[1], P. Kurzweil[2], J. Schottenbauer[3], Ch. Schell[4]

[1]University of Applied Sciences, Electrochemistry Laboratory, Kaiser-Wilhelm-Ring 23, 92224 Amberg, Germany

Abstract: ***Whereas crystalline RuO_2 is well-known in thermally prepared layers, the superior sensitivity dE/dpH of the amorphous oxide prepared by a sol-gel process has not been considered in detail so far. RuO_2 pastes, bound withethyl cellulose, nafion, acrylic resin, and carbon black show Nernstian behavior both in standard pH buffer solutions and in corrosive media. Sintered layers appear to be less sensitive and tend to age. A residual content of chloride influences the properties of the electrode. The impact of the solution resistance on the pH response is obvious during acid-base titrations, which differ considerably from measurements in standard buffer solutions.***

Keywords: amorphous ruthenium dioxide, pH sensor, water quality monitoring, binder

1. Introduction

With respect to the protection of humans and the environment, both experts and broad levels of the population wish to monitor the pH value of tap water, food, beverages [1], urine (pH 4.5−8), saliva (pH ≈7), and blood (pH 7.4 ± 0.05) [2, 3]. Since the 1970s the pH glass electrode has been the method of choice in aqueous solutions providing more or less easy handling, sufficient accuracy and response times. However, for consumer applications, the glass electrode appears to be too complicated, too expensive, too fragile, and too corrosive in strong acids and bases. pH-dependent metal oxidesallow disposable, miniaturized low-cost sensors.

Platinum group metal oxides [4] have been developed for technical DSA electrodes since the 1970s.pH sensorshave been fabricated by thermal decomposition of salt precursors [5], sol-gel processes [6, 7, 8], sputtering [9, 10],electro-deposition [11], and carbon melt oxidation [12]. Screen printing [13, 14] appears to be the most preferred coating technology for small and flexible sensors. PtO_2, Ta_2O_5, TiO_2, PdO, OsO_2, and RhO_2 exhibit good pH sensitivity, although mainly RuO_2 and IrO_2 [15, 16] have been stressed in the literature because of their high conductivity, chemical stability, redox chemistry [17, 26] and ion-exchanging surface [18]. Iridium dioxide can even be used in solutions containing hydrofluoric acid [19].

Ruthenium dioxideis known for its oxygen defect stoichiometry. Due to the "hydrogen intercalation" into theoxide lattice, the electrode potential (equation 2) depends on the proton activity$a_{H^+(aq)}$ in the liquid phase and the oxygen activity$a_{O(s)}$ in the solid phase [20].

$$MO_x + 2z\,H^+ + 2z\,e^- \rightleftharpoons MO_{x-z} + zH_2O \quad (1)$$

$$E = \frac{RT}{F}\ln a_{H^+(aq)} + \frac{RT}{F}\ln a_{O(s)} + \text{const} \quad (2)$$

Once the electrode is immersed in an aqueous electrolyte, protons from the solution penetrate into the porous electrode, diffuse through the defect sites of the rutile lattice, take part in redox reactions and form hydroxide sites (equation 3) [21].The RuO_2 surface is covered with OH-groups having bridged and terminal oxygen atoms (Figure 1).

$$RuO_x(OH)_y + ze^- + zH^+ \rightleftharpoons RuO_{x-z}(OH)_{y+z} \quad (3)$$
$$\text{Simplified: } Ru^{IV}O_2 + e^- + H^+ \rightleftharpoons Ru^{III}O(OH)$$

According to NERNST's equation, and by neglecting the activity of Ru(III) and Ru(IV) in the solid material, the redox potential of the RuO_2 electrode depends directly on the pH value (equation 4) [22].

$$E = E^0 - \frac{RT}{F}\ln\frac{a(Ru^{III})}{a(Ru^{IV})\cdot a(H^+)} =$$
$$= E^0 - \frac{\ln 10\cdot RT}{F}\left(pH + \log\frac{a(Ru^{III})}{a(Ru^{IV})}\right) \quad (4)$$

At 25 °C: $E = E^0 - 0.059\ V\cdot pH$

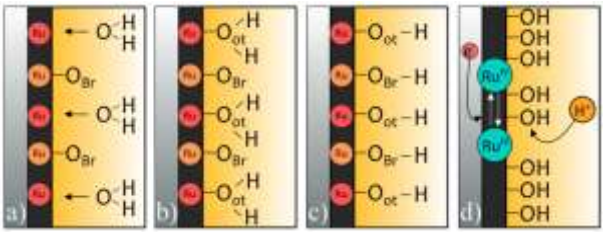

Figure 1: Model of the RuO_2|solution interface: **a,b**disso-ciative adsorption of water, **c** proton displacement during anodic charging, **d** redox reaction involving hydrogen-ions. Ru: ruthenium, O_{Br}: bridged oxygen, O_{ot}: on-top oxygen, H: hydrogen.Modified from [23, 24].

The thermodynamically calculated standard potential of the Ru(III)/Ru(IV) couple amounts toE^0 = 0.94 V SHE [25].The water content of the RuO_2 powder plays an essential role, because a GROTTHUSS-like hopping mechanism of the protons is assumed [26].

This work considers the impact of the crystal structure, the water content, and the binder system on the pH sensitivity of screen-printed ruthenium dioxide sensors.The goal of this

Licensed Under Creative Commons Attribution CC BY

study was to increase the oxygen defect structure of RuO_2 by an increased amount of Ru(III), for example by means of insufficient thermal decomposition of the precursors, or the precipitation of metal oxide hydroxides, respectively.

2. Experimental

We compared RuO_2 sensors made by three different fabrication processes.

Screen printing: The hydrous active material was made by sol-gel synthesis. A 0.5-molarsolution of $RuCl_3{\cdot}x\,H_2O$ in ethanol was precipitated with 1.5-molar KOH solution at least until the mixture reached pH 8. After stirring for one hour at 80 °C, the amorphous RuO_2-gel was purified by repeated washing with deionized water and centrifugation until the pH of the waste water remained constant. The dried oxide was used for paste preparation.The mixing ratios of the binders, ethyl cellulose in terpineol (ET200, Kremer Pigmente), alkyd resin varnish (RAL 3000), thick oil (80014, Wolbring GmbH), epoxy resin (Epoxonic ex 2986), carbon primer (EB-012, Henkel), and Nafion (Ion Power; D520)are given in Table 1. According to Figure 2b, the current collector was printed on soda-limeglass (Ag-Pd paste ESL 9695-G, ElectroScience), dried at 125 °C (15 min), and finally annealed at 600 °C (2 h). The screen-printed active layers (Figure 2c) were dried at150 °C in order to preserve the amorphous structure of hydrous RuO_2. Finally, the silver tracks were sealed with epoxy resin (Figure 2d).

Spray pyrolysis: Titanium foil (Ti) of 0.05 mm thickness (Ankuro Int.) was pretreated with abrasive paper and then degreased with acetone to ensure good adhesion of the oxide layer. A mixture of $RuCl_3{\cdot}x\,H_2O$ (Sigma-Aldrich) dissolved in acetone was decomposed on the substrate at 500 °C (air) for 2 h. Previous investigations revealed the transition temperature of the oxide formation at about 370 °C (Figure 3). Crystalline RuO_2 is formed at 500 °C. The active layer (area 1 cm² and 8.0 mg/cm²) was about 2 µm thick.

Electroplating: Titanium cathodes were coated with ruthenium layers from a 0.04-molar $RuCl_3{\cdot}\ xH_2O$ solution at a current of 5 $mAcm^{-2}$ for 40 and 120 min, and then annealed at 600 °C.

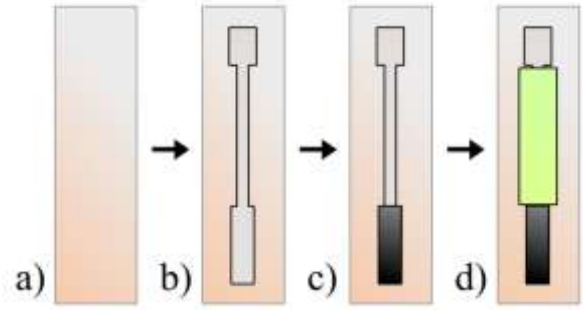

Figure 2: Screen-printing process: **a** degreased substrate, **b.**AgPd conductor, **c.** metal oxide layer (1 cm^2, 8 mg cm^{-2}), **d.**insulating layer.

Instruments and methods.Using a Solartron SI 1287 potentiostat/galvanostat, open circuit potentials and quasi-reversible equilibrium potentials were recorded at a regulated current ($I = 0$) for at least 3 minat room temperature (20 ± 0.5 °C). Standard buffer solutions were pH 4.01 (phthalate), 7.00 (phosphate), and 10.0 (borate). Titrations employed the drop-wise addition of NaOH into 0.5-molar H_2SO_4.The pH was checked using a commercial glass electrode (BlueLine 23 pH). RuO_2 layers were characterized by X-ray diffraction (XRD, RigakuMiniflex 600), electron microscopy (SEM/EDX, Stereoscan LEO 440), and thermogravimetric analysis (TGA, Netzsch 209 F1 Libra) in a platinum-rhodiumcrucible under oxygen atmosphere. The thermal decomposition of the binders was analyzed by thermogravimetric analysis coupled with an FTIR-spectrometer (Bruker Tensor 27) in an aluminum oxide crucible under oxygen atmosphere.

3. Results and Discussion

In the following, the electrochemical properties and the pH sensitivity of amorphous and crystalline RuO_2 layers (prepared by alkaline precipitation, spray pyrolysis, and electroplating) are critically compared.

3.1 Surface properties

The *thermogravimetric analysis* (Figure 3a) shows the $RuCl_3 \rightarrow RuO_2$ transition at about 370 °C. Absorbed and bound water is released below 150−180 °C. Sintering of the particles can be observed above 580 °C. Amorphous $RuO_2{\cdot}xH_2O$, which was won from $RuCl_3$ solution by alkaline precipitation with NaOH, loses most of its water content below 300 to 350 °C. The early water loss below 150 °C corresponds to the formula $RuO_2 \cdot 0.43\ H_2O$. Above 390 °C, more or less water-free RuO_2 is formed.

Crystalline RuO_2 shows defined X-ray diffraction peaks in contrast to the amorphous material (Figure 3b). The ruthenium and oxygen atoms in the bulk material prefer the (110) and (101) planes, whereas (101), (111) and (100) mainly exist on the surface [27]. With the help of the Debye-Scherrer equation, the average crystallite size of 46.0 nm was calculated for powders prepared at 600 °C; the Bragg angle $2\Theta = 28°$ belongs to the crystal orientation (110). $2\Theta = 35°$ corresponds to 36.7 nm (101).

The *SEM images* (Figure 4) show the microporous morphology of crystalline and amorphous RuO_2 powders. With heat treatment, bound water is lost, and the apparent ruthenium content increases. The *EDX analysis* reveals some percent of residual chlorine from the $RuCl_3$ precursor both in the amorphous powder and in the crystalline sample.

Despite repeated washing of the precipitated RuO_2 powder, chloride is still bound in the material. Residual chloride might be of interest for the pH sensitivity. It seems quite conceivable, that some chloride is exchanged by hydroxide in alkaline solutions.Our previous TOF-SIMS studies suggest the formation of Ru-O-Cl clusters [20].

Licensed Under Creative Commons Attribution CC BY

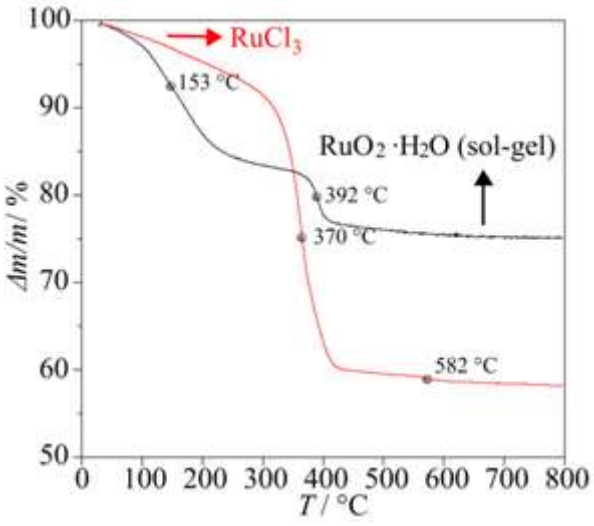

a)

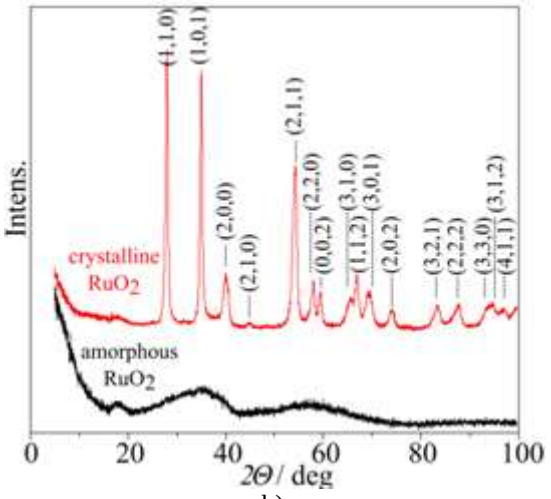

b)

Figure 3: a Thermogravimetry analysis and **b** X-ray diffractograms of crystalline RuO_2 (prepared by decomposition of $RuCl_3$ at 600 °C) and amorphous RuO_2 (by alkaline precipitation, dried at 150 °C).

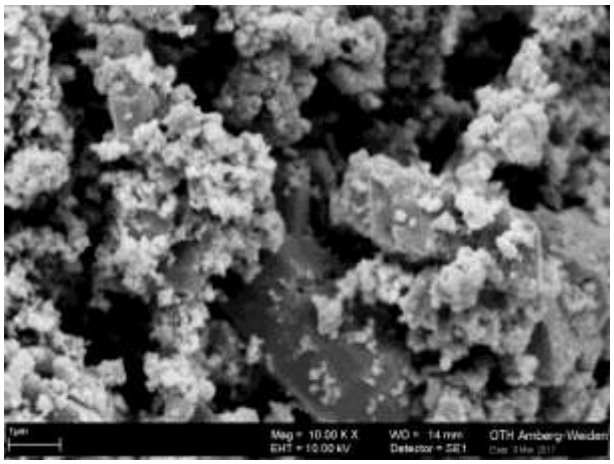

a)

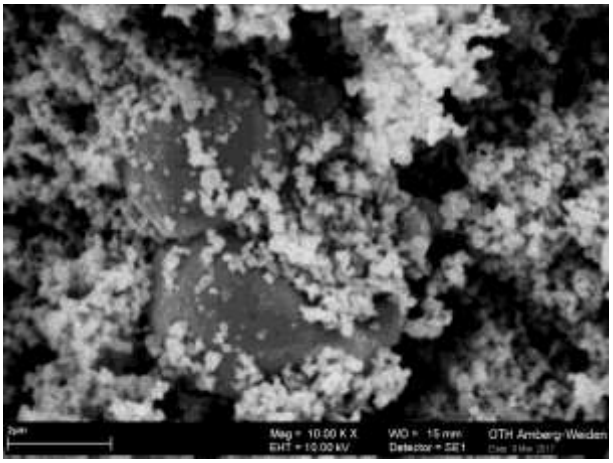

b)

Figure 4: SEM images of microporous RuO_2 prepared by **a**thermolysis at 600 °C, and **b** precipitated RuO_2, dried at 90 °C, 10000-fold magnification.

3.2 Binders

Amorphous RuO_2, won by alkaline precipitation, exhibits a nanoporous structure and includes bound water, which is lost at high temperatures (> 390 °C). In order to maintain the amorphous structure and to guarantee adhesion on the support material, appropriate binders are required, which do not affect the pH sensitivity of RuO_2. Selected binders are allowed to remain in the amorphous layer as long as they improve the mechanical and chemical stability of the sensor. For this reason, several binders were investigated in detail with respect to the thermal decomposition properties.

The thermal behavior of ethyl cellulose and its decomposition products was characterized by TGA-FTIR-coupling in a gas cell (Figure 5a). Ethyl cellulose shows three decomposition steps around 210 °C, 326 °C and 400 °C.At 210 °C, the decomposition products consist mainly of carboxylic acids or esters, such as propanoic acid fragments. Around 326 °C, long-chained ketones and alcohols occur. As well, small amounts of water and carbon dioxide are released. At temperatures above 400 °C, carbon dioxide is the principal decomposition product of the binder (Figure 6). Above 425 °C, the binder is completely decomposed (mass loss 100 %).

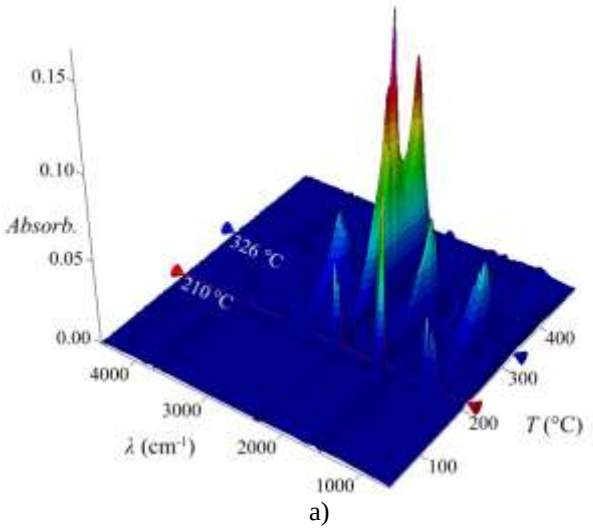

a)

Licensed Under Creative Commons Attribution CC BY

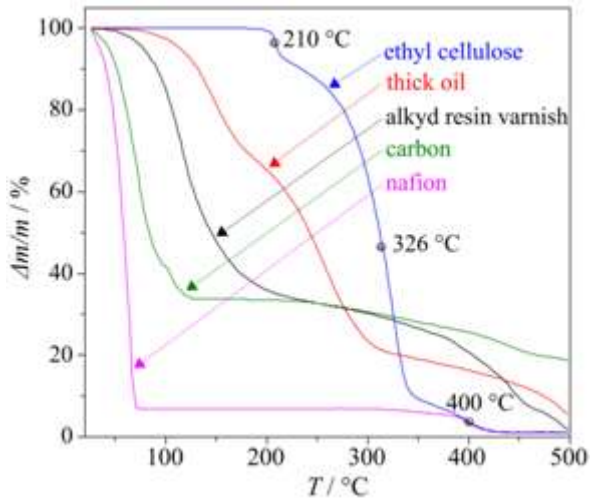

b)

Figure 5: a Thermogravimetric analysis coupled with infrared spectrometry (FTIR-TGA) of ethyl cellulose between 30 °C and 500 °C at 10 °C/min in oxygen atmosphere. **b**TGA analysis of different binders at 10 °C/min.

The thermal behavior of Nafion in 5 wt% ethanolic solution is coined by the evaporation of the solvent (Figure 5b). The polymer decomposes more or less completely at temperatures around 425 °C.

Thick oil and alkyd resin varnish tend to decompose completely above 500 °C.

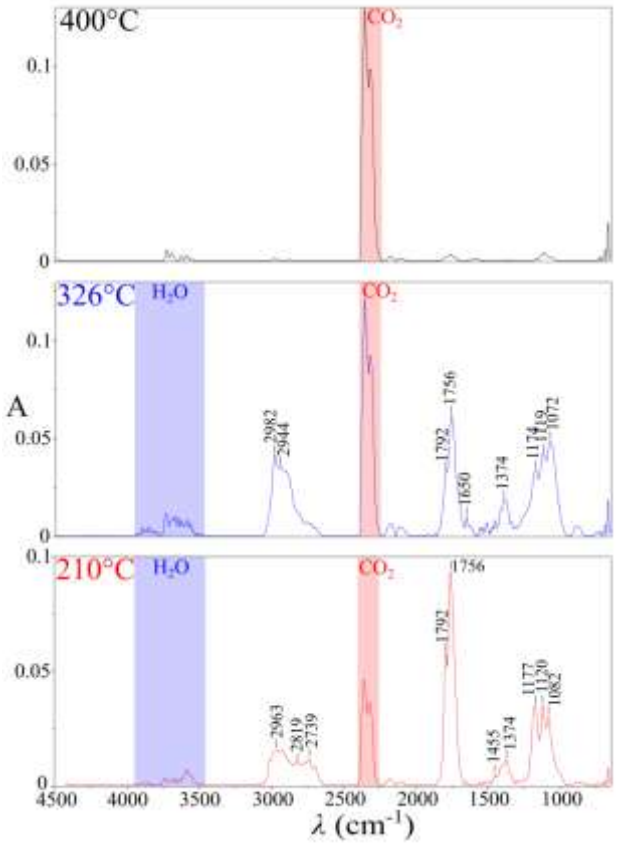

Figure 6: Infrared spectra of the gaseous decomposition products of ethyl cellulose at different temperatures.

In contrast, the carbon binder loses its solvent at about 125 °C. The carbon particles remain in the active material and improve the conductivity of the electrode. Heated at 500 °C, the carbon binder still contains 19 wt% of its initial mass.

We conclude that 150 °C is an adequate drying temperature for amorphous RuO_2. Some residual amount of binder improves the mechanical stability of the active layer.

3.3 Sensitivity in buffer solutions

The binder plays an important role for the practical sensitivity of the sensor. Table 1 compiles the slopes d*E*/d*p*H of RuO_2 electrodes measured in standard buffer solutions. Preferably, the amorphous RuO_2/*ethyl cellulose* sensor (20:80) exhibits a linear Nernstian response (59 mV/pH). This sensitivityis confirmed by the data of MANJAKKAL et al. for screen printed sensors based on crystalline RuO_2 (Table 2). The organic binder decomposes at around 300 to 400 °C. Heat treatment of $RuCl_3$ at 500 °C generates a crystalline RuO_2 layer of low active surface area showing a sensitivity of 52 mV/pH. During aging, the sensitivity of such a thermal Ti/RuO_2 electrode may increase up to 76 mV/pH; and the electrode standard potential drifts.

Acrylic resin appears to be useful for sensors; we foundNERNSTian behavior. In contrast to that, epoxy resin appears to be inappropriate for flat sensors, because it peels off. 'Thick oil' evaporates and decomposes between 100 to 250 °C, so that small amounts are still present in the active layer dried at 150 °C. This explains the undesired sensitivity of 64 mV/pH. Unfortunately, the sensor is not long-term stable, and the layer dissolves visibly after a few measurements.

Nafion [28] seems to be a useful binder for metal oxide powders because of its good proton conductivity. Its sensitivity is low compared with ethyl cellulose.Unfortunately, Nafion tends to increase the sheet resistance (Figure 7). Despite long response times, Nafion improves the selectivity against interfering ions, although chloride ions can penetrate the membrane [29, 30].

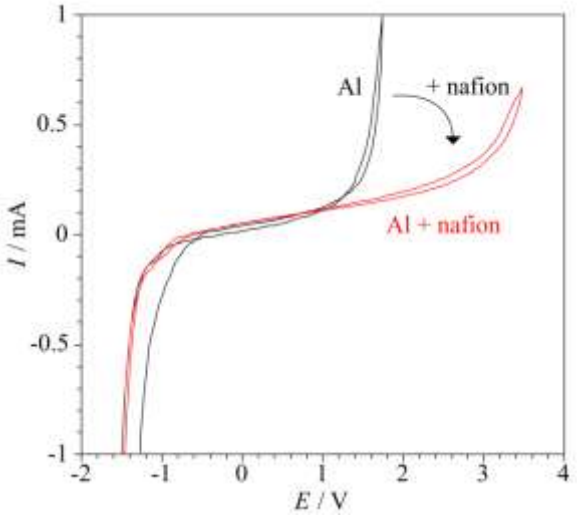

Figure7: Increasing contact resistance of an aluminum sheet coated with Nafion in 0.1-molar sulfuric acid at 20 °C (area 6.25 cm², counter electrode: platinum; reference

Licensed Under Creative Commons Attribution CC BY

electrode: silver rod; scan rate: 100 mV/s).

Carbon. With investigating different compositions of porous carbon and RuO_2, surprisingly, the pH response drops with increasing amount of RuO_2(Table 1). In order to exclude interfering effects, the sensitivities of the bare substrates and binders were tested separately (Table 3).

Indeed, the substrate plays a minor role for the pHresponse, because the sensor is coated sufficiently thick with RuO_2.

The ***electroplated sensors***(without binder) suggest that chemisorbed and bound water is incorporated in the active layer [31]. The sensitivity d*E*/d*p*H amounts to just half the value of the amorphous RuO_2 hydrate, because the electrodeposited layers were annealed at 600 °C, whereby crystalline RuO_2 is generatedThe loss of sensitivity corresponds to the mass increase around 576 °C in the thermogravimetric analysis. This oxidation of electro-deposited ruthenium between 430 and 480 °C was observed byMARIJAN et al. [32] as well

We conclude that the sensitivity of a RuO_2 sensor can be improved by amorphous oxide. Binders, except ethyl cellulose and acrylic varnish, reduce the sensitivity (see Table 1). The response of the metal oxide in carbon (RuO_2:C = 20:80) comes close to the optimum pH-response known from the glass electrode.The sensitivity of the electrodeposited layers suggest that two electrons ($z = E/59$ mV ≈ 2) are involved in the potential determining step, whereas the amorphous oxide perfectly utilizes the $RuO(OH)/RuO_2$ couple (z = 1). Virgin electrodes prepared by thermolysis show sensitivities around 52 mV/pH ($z \approx 1$). However, insulating binders such as epoxy resin cause low sensitivity (18 mV/pH). An increase in sensitivity was achieved by the addition of activated carbon [33].

Table 1: RuO_2 electrodes manufactured with different binders in pH standard buffer solutions at 20 °C.

Type	Amorphous oxide (from precipitation and dried at 150 °C)									Crystalline oxide (thermolysis at 500 °C)		Electrodeposited oxide (annealed at 600 °C)	
Binder	RuO_2 / ethyl cellulose	RuO_2 / acrylic varnish	RuO_2 / thick oil	RuO_2 / epoxy resin	RuO_2 / carbon	RuO_2 / carbon	RuO_2 / carbon	RuO_2 / carbon / nafion	RuO_2 / nafion	(1) Ti/ RuO_2 aged	(2) Ti/ RuO_2 pristine	RuO_2 40 min	RuO_2 120 min
mixture wt%	20:80	50:50	50:50	25:75	20:80	40:60	80:20	80:20:10	20:80	–	–	–	–
Sensitivity mV/pH	–59.0	–56.5	–64.6	–17.8	–48.8	–41.5	–36.1	–40.7	–41.5	–75.9	–52.0	–23.7	–27.3
Linearity R^2	0.996	0.999	0.906	0.904	0.981	0.992	0.986	0.995	0.954	0.999	0.981	0.974	0.988
E^0 / mV vs. Ag|AgCl	670	661	810	710	524	592	623	642	592	882	605	348	400

Table2: Literature data:pH response of crystalline RuO_2 composites with ethyl cellulose in terpineol

	RuO_2	RuO_2:TiO_2	RuO_2	RuO_2:SnO_2	RuO_2:Ta_2O_5	RuO_2:Ta_2O_5
Ref.	[a]	[b]	[c]	[d]	[e]	[e]
w / %	–	70:30	–	70:30	70:30	30:70
T / °C	850	900	850	900	900	900
pH-range	2-10	2-12	2-10	2-10	2-12	2-12
mV/pH	–57	–56.1	–60.7	–56.5	–56.1	–35

[a] L. Manjakkal, K. Cvejin, J. Kulawik, K. Zaraka, D. Szwagierczak, A low-cost pH Sensor Based on RuO_2 Resistor Material, *Nano Hybrids 5* (2013) 1–15.
[b] L. Manjakkal, K. Cvejin, J. Kulawik. K. Zaraska, D. Szwagierczak, R. P. Socha, Fabrication of thick film sensitive RuO_2-TiO_2 and Ag/AgCl/KCl reference electrodes and their application for pH measurements, *Sensors and Actuators B 204* (2014) 57–67.
[c] L. Manjakkal, K. Cvejin, J. Kulawik. K. Zaraska, D. Szwagierczak, The Effect of Sheet Resistivity and Storage Conditions on Sensitivity of RuO_2 Based pH Sensors, *Key Engineering Materials Vol. 605* (2014) 457–460.
[d] L. Manjakkal, K. Cvejin, J. Kulawik, K. Zaraka, D. Szwagierczak, G. Stojanovic, Sensing mechanism of RuO_2-SnO_2 thick film pH sensors studied by potentiometric method And electrochemical impedance spectroscopy, *Journal of Electroanalytical Chemistry 759* (2015) 82–90.
[e] L. Manjakkal, K. Zaraska, K. Cvejin, J. Kulawik, D. Szwagierczak, Potentiometric RuO_2-Ta_2O_5 pH sensors fabricated using thick film and LTCC technologies, *Talanta 147* (2016) 233–240.

Table 3: pH-response of bare substrates and binders vs. Ag|AgCl|KCl in buffer solutions (pH 4, 7, and 10) at 20 °C

Electrode	Ag/Pd current collector	Ag/Pd + nafion	Ag/Pd + carbon	Ti (500 °C)
mV/pH	−13.3	−13.9	−15.0	−46.4
R^2	0.981	0.970	0.881	0.999

3.4 Hysteresis and drift

Known problems of RuO_2 electrodes are (i) hysteresis, i.e., divergent potentials in the same solution after measurements in differently concentrated solutions, and (ii) potential drift, i.e., the slow nonrandom change of the output voltage in time.Table 4 demonstrates the superior stability of the carbon-based binder in contrast to ethyl cellulose. Depending on the preparation procedure, hysteresis and drift values of RuO_2 sensors range between 3 and 30 mV (Figure 8). In acid solution, hysteresis is lower than in alkaline solution.

Licensed Under Creative Commons Attribution CC BY

This may be due to the fact that the equilibrium potential is reached faster in acid solution, whereas in alkaline solution higher oxidation states and soluble species are stabilized.

Hysteresis and potential drift directly influence the sensitivity of the electrodes. At pH changes of 4→7→10, the sensitivity of the ethyl cellulose sensor was –54 mV/pH ($R^2 = 0.996$), whereas at pH 7→4→10 it dropped to −52 mV/pH ($R^2 = 0.996$). Carbon-bound RuO_2 electrodes decrease from −49 mV/pH ($R^2 = 0.972$) to −48 mV/pH ($R^2 = 0.992$). Unfortunately, the pH response lies not far above the range of thermal noise, $RT/F \approx 25$ mV.

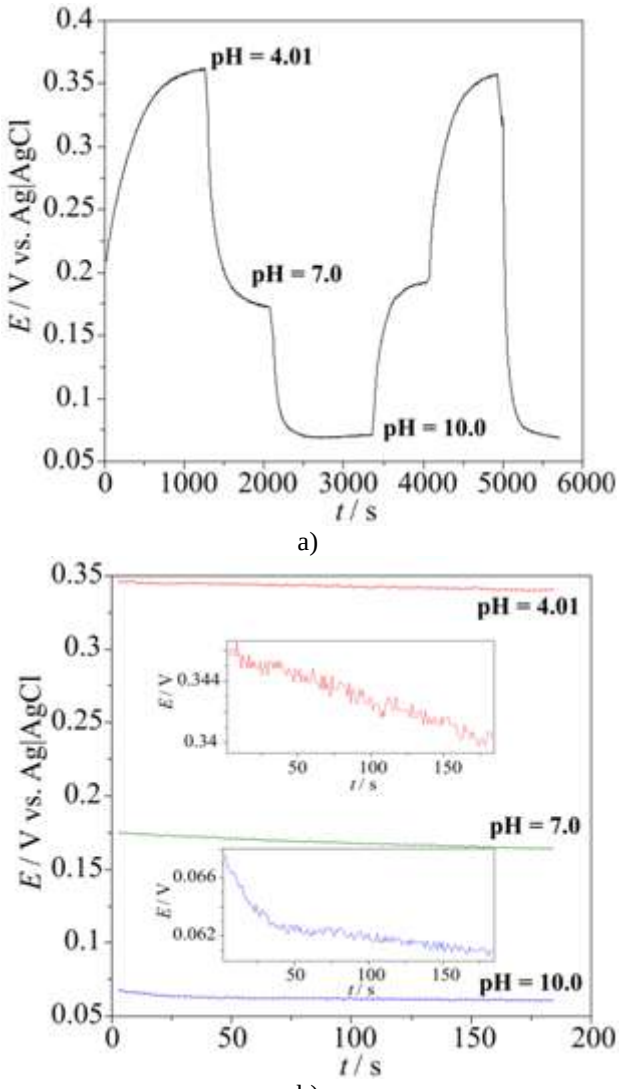

Figure 8: a Hysteresis and **b** potential drift of a RuO_2sensor (amorphous RuO_2:C = 20:80) in buffer solutions.

Table 4: Hysteresis and potential drift (during 180 s) of RuO_2 sensors measured in buffer solutions

Binder	Ethyl cellulose		Carbon	
pH	hysteresis (mV)	Drift (mV/h)	Hysteresis (mV)	Drift (mV/h)
4	18.3	16	4.2	114
7	18.6	546	19.3	208
10	9.7	90	none	132

3.5 Sensitivity during acid-base titration

In practical use, metal oxide electrodes must show the same sensitivity in different media. For this reason, we investigated RuO_2 electrodes bound with (i) ethyl cellulose and (ii) carbon during the titration of 0.5-molar sulfuric acid by dropwise addition of sodium hydroxide solution (Table 5). Between each pH measurement, the solution was mixed using a magnetic stirrer for about 2 minutes (300 min^{-1}). The pH values were checked by a conventional glass electrode. The open-circuit potential (OCP) inFigure 9 was measured by the help of a galvanostat at the regulated current $I = 0$ for at least 5 min.

The sensitivity lies at an average value of $–32 \pm 4$ mV/pH, and is thus lower than in buffer solutions. A drastic loss of the sensitivity is observed in tap water. Originally, we assumed that the low sensitivity was caused byconductivity alterationsduring the neutralization reaction. However, the electrolyte resistance of the reaction $H_2SO_4 + 2\,NaOH \rightleftharpoons Na_2SO_4 + 2\,H_2O$ is greatest at pH 7. Measurements in diluted acids (1, 0.1, 0.01, and 0.001-molar H_2SO_4 versus 0.001, and 0.01-molar NaOH) rendered almost the same OCP (Table 5). The same observations we made with carbon-based electrodes. Since the titration curve is not a straight line, we determined the sensitivity in individual pH ranges. In strongly acid and strongly alkaline solution, qualitatively the same pH responsewas observed as in buffer solutions. However, the sensitivity reaches a minimum in the neutral range at pH 6 to 9, especially in tap water. Similar to the electrodes with binders, the sensitivity of the binder-less electrodes decreases by 10 to 25 mV/pH, when the pH was not measured in standard buffer solutions, but during a neutralization reaction.

We conclude that the conductivity of the solution is of importance for the slope d*E*/d*p*H. Since tap water has a high resistance compared with the neutralized mixture of H_2SO_4 and NaOH, the sensitivity in water is considerably lower. The binder resistance seems to play a minor role for the loss of sensitivity in "real solutions".RuO_2 bound with ethyl cellulose is usable in a pH range between 0 and 14.

Screen-printed sensors do not show any additional activity in strong acids (pH < 0). The rest potential (OCP)equals 520 mV in 5-molar H_2SO_4 (negative pH −1.5), about 535 mV in 3-molar H_2SO_4, and about 534 mV in 1-molar H_2SO_4 (pH −0.48)vs. Ag|AgCl|KCl.

Figure 9: Rest potential (OCP) of a RuO_2sensor (20 % amorphous RuO_2, 80 % ethyl cellulose) in standard buffers

Licensed Under Creative Commons Attribution CC BY

and real aqueous solutions during acid-base titration at 20 °C. pH controlled by a commercial glass electrode.

Table 5: Sensitivity of RuO_2 electrodes during titration of sulfuric acid with NaOH, and in tap water, versus Ag|AgCl at 20 °C.Standard solutions were prepared by dilution: 1, 0.1,0.01,0.001, 0.0001-molar H_2SO_4, and 0.001, 0.01-molar NaOH.

	buffer	1st titration	2nd titration	tap water	3rd titration	Standard buffer solution
Binder	Ethyl cellulose (RuO_2:ethyl cellulose = 20:80)					
points	3	10	9	3	3	7
pH-range	4…10	0…12	1…13.5	3…10	2…9	0…9.5
mV/pH	–59.0	–27.7	–33.5	–10.0	–35.6	–30.4
R^2	0.996	0.909	0.979	0.936	0.872	0.881
E (mV)	670	424	501	285	461	459
mV/pH pH 0−3		–56.2	–58.2		pH 1-6: –44 .4	
pH 3−6		–37.8				
pH 6−9		–7.1				
pH 9−12		–19.4				
pH 6−11					–19.9	
pH 11−13					−52.6	
Binder	Carbon (RuO_2:C = 20:80)					
points	3	10	9	3	3	
mV/pH	–48.8	–18.5	–35.6	+6.5	–27.2	
R^2	0.981	0.771	0.980	0.983	0.610	
E (mV)	524	304	474	125	452	
	No binder					
pH-range	4 to 10	4 to 10	3 to 10			
mV/pH	–76…−52	–50.4	–40.8			
R^2	0.999	0.999	0.989			
E (mV)	605…882	612	540			

3.6 Response time

We define the response time as the time to reach 90 % of the equilibrium potentialaccording to HUANG et al. [34], The response of amorphous RuO_2:ethyl cellulose (20:80) and RuO_2:carbon (20:80) was measured in buffer solutions in the order: pH 4→7→10→7→4→10. In contrast to sintered layers, we expected extended response times due to the incompletely decomposed binders. On the other hand, binders improve the adhesion and thus the lifetime of the RuO_2layers. Ethyl cellulose required less than 2 min in acidic and less than 3 min in alkaline solutions, whereas the carbon-based sensor exhibits an average response time of less than 4 min.

During acid-base titration, the sensors bound with ethyl cellulose and carbon work faster than in buffer solutions. RuO_2/ethyl cellulose reaches its open-circuit potential within lees than 1 min in acid and alkaline solutions, whereas the carbon-based electrode needs < 10 s (acid) and < 2 min (alkaline), respectively. The fast response during titration may be due to the higher number of surface charges, and the better conductivity of the solution (≈ 65 mS/cm for buffer solutions and about 40 to 380 mS/cm during titration). In acid solutions, the drift behavior is more pronounced for both sensors: 230 mV/h (ethyl cellulose) and 210 mV/h (carbon) at pH 1. The drift in alkaline solutions is about 32 mV/h (ethyl cellulose) and 46 mV/h (carbon primer) at pH = 10.

4. Conclusions

Until, one day, miniaturized low cost pH sensors based on metal oxides might be able to replace the glass electrode in anysolution, some obstacles considered in this paper have to be overcome. In pH buffer solutions, RuO_2 electrodes respond in nearly the same ideal way as the glass electrode does. Challenges arise in real solutions with undefined ionic strength.

1) Amorphous RuO2 bound with ethyl cellulose shows ideal sensitivity (−59 mV/pH, 25 °C). At drying temperatures below 150 °C, enough Ru(III) in the material provides sufficient redox activity for pH sensitivity. Amorphous RuO2 was won from RuCl3by alkaline precipitation with NaOH.
2) The sensitivity dE/dpH of carbon-bound electrodes drops with increasing RuO2 content. Obviously, a higher number of charge carriers is involved in the conversion of Ru(III) to Ru(IV), when RuO2 is finely dispersed at the electrode surface, whereas the bulk material behaves inactive. The potential determining step of the amorphous oxide perfectly utilizes the RuO(OH)/RuO2 couple (z = 1).
3) With sintering RuO2 electrodes up to 800 °C, the particles agglomerate and lose water, so that electrodes prepared by thermolysis show the low sensitivity of crystalline RuO2(compared with the amorphous hydrate).Virgin electrodes prepared by thermolysis show sensitivities around 52 mV/pH (z ≈ 1).
4) Both the mechanical stability and the sensitivity dE/dpH of RuO2layers can be improved by using a Nafion binder. A bare Nafion layer (e. g. on a Ag/Pd current collector) does not create any pH sensitivity. RuO2 works as the proton-selective component in the polymer-composite electrode.
5) RuO2 electrodes respond more quickly during acid-base titrations than in buffer solutions. Unfortunately, sensitivity deviates from59 mV/pH because the solution resistance changes continuously (maximum at pH 7). This surprising difference between real solutions and "ideal" pH buffers requires further studies with respect to

Licensed Under Creative Commons Attribution CC BY

the ionic strength of the solution. We suggest that RuO2 indicates the real proton activity a(H+, aq) at the metal oxide/electrolyte interface.

Up to now, pH values can only be compared in media of the same ionic strength and the same solvent. Absolute pH measurements in any medium have not been feasible so far. Present pH meters must be calibrated against at least two buffer solutions. The primary method for pH measurement, the so-called HARNED cell [35, 36], employing a hydrogen electrode (platinum aerated by dry hydrogen at atmospheric pressure) and a silver-silver chloride electrode, requires the knowledge of activity coefficients that usually are completely unknown for technical media. The future will show whether platinum metal oxide might open up novel ways of pH measurement.

References

[1] W. Lonsdale, M. Wajrak, K. Alameh, Manufacture and application of RuO_2 solid-state metal-oxide pH sensor to common beverages, *Talanta 180* (2018) 277-281.
[2] F. F. Sander, *The acid-base balance of the human organism* (in German), Hippokrates, Stuttgart 1999.
[3] M. Yuqing, C. Jianrong, F. Keming, New technology for the detection of pH.*J. Biochem. Biophys. Methods* 63 (2005) 1–9.
[4] S. Trasatti, *Electrodes of conductive metallic oxides*, Elsevier, Amsterdam 1980.
[5] S. Chalupczok, P. Kurzweil, H. Hartmann, Impact of Various Acids and Bases on the Voltammetric Response of Platinum Group Metal Oxides, *International Journal of Electrochemistry*, vol. 2018, Article ID 1697956, 6 pages, 2018. doi:10.1155/2018/1697956.
[6] M. Guglielmi, P. Colombo, V. Rigato, G. Battaglin, A. Boscolo-Boscoletto, A. DeBattisti, Compositional and Microstructural Characterization of RuO2-TiO2 Catalysts Synthesized by the Sol-Gel Method, *J. Electrochem. Soc.* 139 (1992) 1655-1661.
[7] L. A. Pocrifka, C. Gonçalves, P. Grossi, P.C. Colpa, E.C. Pereira, *Sens. Actuators 113* (2006) 1012–1016.
[8] G. M. da Silva, S. G. Lemos, L. A. Pocrifika, P. D. Marreto, A. V. Rosario, E. C. Pereira, Development of low-cost metal oxide pH electrodes based on the polymeric precursor method, *Anal. Chim.Acta616* (2008) 36–41.
[9] Y. H. Liao, J. C. Chou, Preparation and characteristics of ruthenium dioxide for pH array sensors with real-time measurement system, *Sens. Actuators B128* (2008) 603–612.
[10] A. Saradinejad, D. K. Maurya, K. Alameh, The pH Sensing Properties of RF Sputtered RuO2 Thin-Film prepared using different Ar/O2 Flow Radio, *Materials8* (2015) 3352–3363.
[11] P. Steegstra, E. Ahlberg, Influence of oxidation state on the pH dependence of hydrous iridium oxide films, *Electrochim.Acta 76* (2012) 26–33.
[12] M. Wang, S. Yao, M. Madou, A long-term stable iridium oxide pH electrode, *Sens. Actuators B81* (2002) 313–315.
[13] R. Koncki, M. Mascini, Screen-printed ruthenium dioxide electrodes for pH measurements, *Anal.Chim.Acta351* (1997) 143–149.
[14] L. Manjakkal, K. Cvejin, J. Kulawik. K. Zaraska, D. Szwagierczak, R. P. Socha, Fabrication of thick film sensitive RuO2-TiO2 and Ag/AgCl/KCl reference electrodes and their application for pH measurements, *Sens. Actuators B* 204 (2014) 57–67.
[15] A. Fog, R. P. Buck, Electronic semiconducting oxides as pH sensors, *Sens. Actuators5* (1984) 137–146.
[16] S. Głab, A. Hulanicki G. Edwall, F. Ingman, Metal-Metal Oxide and Metal Oxide Electrodes as pH Sensors, *Crit. Rev. Anal. Chem. 21* (2006) 29–47.
[17] S. E. Livingstone, The Chemistry of Ruthenium, Rhodium, Palladium, Osmium, Iridium and Platinum, in: *Inorganic Chemistry*, Vol. 25, Pergamon Press: New York 1975.
[18] P. Kurzweil, Metal Oxides and Ion-Exchanging Surfaces as pH Sensors in Liquids: State-of-the-Art and Outlook, *Sensors 9* (2009) 4955–4985.
[19] H. L. Hitchman, S. Ramanathan, Potentiometric Determination of Proton Activities in Solutions Containing Hydrofluoric Acid Using Thermally Oxidized Iridium Electrodes, *Analyst116* (1991) 1131–1133.
[20] H. N. McMurray, P. Douglas, D. Abbot, Novel thick-film pH sensors based on ruthenium dioxide-glass composites, *Sens. Actuators B28* (1995) 9–15.
[21] (a) S. Trasatti, P. Kurzweil, Electrochemical supercapacitors as versatile energy stores, *Platinum Metals Rev.* 38 (1994) 46-56. – (b) S. Trasatti, Physical electrochemistry of ceramic oxides, *Electrochim.Acta*36 (1991) 225-241.
[22] P. Kurzweil, Precious Metal Oxides for Electrochemical Energy Converters: Pseudocapacitance and pH Dependence of Redox Processes, *J. Power Sources190* (2009) 189–200.
[23] H. Over, Surface Chemistry of Ruthenium Dioxide in Heterogeneous Catalysis and Electrocatalysis: From Fundamental to Applied Research, *Chem. Rev. 112* (2012) 3356–3426.
[24] S. Chalupczok, P. Kurzweil, H. Hartmann, C. Schell, The Redox Chemistry of Ruthenium Dioxide: A Cyclic Voltammetry Study – Review and Revision, *International Journal of Electrochemistry*, vol. 2018, Article ID 1273768, 15 pages, doi:10.1155/2018/1273768.
[25] D. Galizzioli, F. Tantardini, S. Trasatti, Ruthenium dioxide: a new electrode material. I. Behaviour in acid solutions of inert electrolytes, *J. Appl. Electrochem.4* (1974) 57–67; II.Non-stoichiometry and energetics of electrode reactions in acid solutions, *J. Appl. Electrochem.5* (1975) 203–214.
[26] N. Agmon, The Grotthus mechanism, *Chemical Physics Letters 244* (1995) 456–462.
[27] T. Hepel, F. Pollak, W. E. Grady, Effect of Crystallographic Orientation of Single-Crystal RuO2 Electrodes on the Hydrogen Adsorption Reactions, *J. Electrochem. Soc.: Solid-State science and technology 131* (1984) 2094–2100.
[28] K. A. Mauritz, R. B. Moore, State of Understanding of Nafion, *Chem. Rev. 104* (2004) 4535–4585.
[29] S. A. M. Marzouk, Improved Electrodeposited Iridium Oxide pH Sensor Fabricated on Etched Titanium Substrates, *Anal. Chem. 75* (2003) 1258–1266.

Licensed Under Creative Commons Attribution CC BY

[30] D. O'Hare, K. H. Parker, C. P. Winlove, Metal-metal oxide pH sensors for physiological application, *Medical Engineering & Physics 28* (2006) 982–988.
[31] M. Vuković, D. Čukman, Electrochemicalquarz crystal microbalance study of electrodeposited ruthenium, *J. Electroanal. Chem. 474* (1999) 167–173.
[32] D. Marijan, D. Cukman, M. Vukovic, M. Milun, Anodix stability of electrodeposited ruthenium: galvanostatic, thermogravimetric and X-ray photoelectro spectroscopy studies, *J. mat. science 30* (1995) 3045–3049.
[33] S. Huang, Y. Jin, Z. Su, Q. Jin, J. Zhao, Performance of surface renewable pH electrodes based on RuO2-graphite-epoxy composites, *Analytical Methods 9* (2017) 1650–1657.
[34] W.-D. Huang, H. Cao, S. Deb, M. Chiao, J.C. Chiao, A flexible pH sensor based on the iridium oxide sensing film, *Sens. Actuators A169* (2011) 1–11.
[35] H. S. Harned, B. B. Owen, *The Physical Chemistry of Electrolytic Solutions*; Chap. 14, Reinhold: New York, 1958.
[36] P. Fisicaro, E. Ferrara, E. Prenesti, S Berto, Role of the activity coefficient in the dissemination of pH: comparison of primary (Harned cell) and secondary (glass electrode) measurements on phosphate buffer considering activity and concentration scale, *Anal. Bioanal. Chem.383* (2005) 341 – 348.

Licensed Under Creative Commons Attribution CC BY